World Journal of

Meta-Analysis

World Journal of
Meta-Analysis

Contents

MINIREVIEWS

Contents

ABOUT COVER

Editorial Board Member of *World Journal of Meta-Analysis*, Hong-Xia Wang, MD, PhD, Attending Doctor, Deaprtment of Oncology, Shanghai Renji Hospital, Shanghai Jiaotong University, School of Medicine, Shanghai 200001, China

AIM AND SCOPE

World Journal of Meta-Analysis (*World J Meta-Anal*, *WJMA*, online ISSN 2308-3840, DOI: 10.13105) is a peer-reviewed open access academic journal that aims to guide clinical practice and improve diagnostic and therapeutic skills of clinicians, with a specific focus on meta-analysis, systematic review, mixed-treatment comparison, meta-regression, overview of reviews.

WJMA covers a variety of clinical medical fields including allergy, anesthesiology, cardiac medicine, clinical genetics, clinical neurology, critical care, dentistry, dermatology, emergency medicine, endocrinology, family medicine, gastroenterology and hepatology, geriatrics and gerontology, hematology, immunology, infectious diseases, internal medicine, obstetrics and gynecology, oncology, ophthalmology, orthopedics, otolaryngology, pathology, pediatrics, peripheral vascular disease, psychiatry, radiology, rehabilitation, respiratory medicine, rheumatology, surgery, toxicology, transplantation, and urology and nephrology, while maintaining its unique dedication to systematic reviews and meta-analyses.

INDEXING/ABSTRACTING

World Journal of Meta-Analysis is now indexed in Emerging Sources Citation Index (Web of Science).

FLYLEAF

EDITORS FOR THIS ISSUE

Diffusion tensor imaging beyond brains: Applications in abdominal and pelvic organs

Yu-Ting Wang, Ying-Chun Li, Wei-Fang Kong, Long-Lin Yin, Hong Pu

Yu-Ting Wang, Ying-Chun Li, Wei-Fang Kong, Long-Lin Yin, Hong Pu, Department of Radiology, Sichuan Academy of Medical Sciences and Sichuan Provincial People's Hospital, Chengdu 610072, Sichuan Province, China

Author contributions: Wang YT designed the main ideas; Li YC, Kong WF, Yin LL and Pu H helped collect relevant data; Wang YT wrote the paper.

Conflict-of-interest statement: The authors declare no conflicts of interests.

Open-Access: This article is an open-access article which was selected by an in-house editor and fully peer-reviewed by external reviewers. It is distributed in accordance with the Creative Commons Attribution Non Commercial (CC BY-NC 4.0) license, which permits others to distribute, remix, adapt, build upon this work non-commercially, and license their derivative works on different terms, provided the original work is properly cited and the use is non-commercial. See: http://creativecommons.org/licenses/by-nc/4.0/

Manuscript source: Invited manuscript

Correspondence to: Yu-Ting Wang, MD, Department of Radiology, Sichuan Academy of Medical Sciences and Sichuan Provincial People's Hospital, No. 32, Section 2, 1st Ring Road (West), Chengdu 610072, Sichuan Province, China. wangyuting_330@163.com
Telephone: +86-28-87394280

Received: December 28, 2016
Peer-review started: December 31, 2016
First decision: March 27, 2017
Revised: April 7, 2017
Accepted: April 23, 2017
Article in press: April 24, 2017
Published online: June 26, 2017

Abstract

Functional magnetic resonance imaging (MRI) provided critical functional information in addition to the anatomic profiles offered by conventional MRI, and has been enormously used in the initial diagnosis and followed evaluation of various diseases. Diffusion tensor imaging (DTI) is a newly developed and advanced technique that measures the diffusion properties including both diffusion motion and its direction *in situ*, and has been extensively applied in central nerve system with acknowledged success. Technical advances have enabled DTI in abdominal and pelvic organs. Its application is increasing, yet remains less understood. A systematic overview of clinical application of DTI in abdominal and pelvic organs such as liver, pancreas, kidneys, prostate, uterus, *etc.*, is therefore presented. Exploration of techniques with less artifacts and more normative post-processing enabled generally satisfactory image quality and repeatability of measurement. DTI appears to be more valuable in the evaluation of diffused diseases of organs with highly directionally arranged structures, such as the assessment of function impairment of native and transplanted kidneys. However, the utility of DTI to diagnose focal lesions, such as liver mass, pancreatic and prostate tumor, remains limited. Besides, diffusion of different layers of the uterus and the fiber structure disruption can be depicted by DTI. Finally, a discussion of future directions of research is given. The underlying heterogeneous pathologic conditions of certain diseases need to be further differentiated, and it is suggested that DTI parameters might potentially depict certain pathologic characterization such as cell density. Nevertheless, DTI should be better integrated into the current multi-modality evaluation in clinical practice.

Key words: Functional magnetic resonance imaging; Diffusion tensor imaging; Abdomen; Pelvis; Kidney

Core tip: As a newly developed and advanced technique of functional magnetic resonance imaging, diffusion tensor imaging (DTI) measures the diffusion properties

including anisotropy. After its successful application in brains, technical advances have now enabled DTI in abdominal and pelvic organs. We herein give a systematic overview of clinical application of DTI in abdominal and pelvic organs such as liver, pancreas, kidneys, prostate, uterus, *etc*. DTI appears to be more valuable in the evaluation of diffused diseases of organs with highly directionally arranged structures, such as the assessment of function impairment of native and transplanted kidneys. However, the utility of DTI to diagnose focal lesions remains limited. It is suggested that DTI parameters might potentially depict certain pathologic characterization such as cell density.

INTRODUCTION

As conventional magnetic resonance imaging (MRI) offers excellent anatomic information and has gained considerable success in the disease diagnosis throughout the body, functional assessment becomes available with the rapid development of related techniques. Considering the radiation caused by nuclear medicine examinations and the risk of nephrogenic systemic fibrosis in enhanced MRI scans, unenhanced MRI techniques have gained special clinic interest[1]. Diffusion-weighted imaging (DWI), which uses motion of intrinsic water molecules as genuine contrast was explored, then diffusion tensor imaging (DTI) made a step further and detects diffusion properties along at least six different directions, from which the main diffusion direction and the degree of diffusion anisotropy can be calculated[2]. A frequently used index to measure diffusion anisotropy is the fractional anisotropy (FA), ranges from 0 (isotropic: No preferred direction) to 1 (full anisotropy: Only one direction)[3]. The collected data can be converted to gray-scaled FA-maps, color-coded orientation image, and furthermore, tractography that enables 3D reconstruction[4]. Such data provided unique insight into the tissue microstructure, especially those with highly direction preference.

DTI has been traditionally applied to the brain, where tractography was developed to visualize white matter fiber bundles, and microstructural injuries of white matter fiber tracts were quantified[5]. It has been extensively used in the evaluation of brain tumor, injury, degeneration, *etc*.[5-7]. Although abdominal and pelvic MRI encountered some problems such as motion artifacts when first introduced, various techniques such as respiratory triggering and breath-hold imaging have sufficiently improved the image quality[8,9]. Accordingly, the utility of DTI is rapidly extending. However, DTI of

abdomen and pelvis was relatively inadequately understood. Furthermore, DTI of various organs may have different clinical emphasis and challenges due to these distinct structures and physiologies. This review aims to give a systematic overview of clinical application of DTI in abdominal and pelvic organs such as liver, pancreas, kidneys, uterus, prostate, *etc*., and discuss potential future research directions of the above-mentioned issues.

DTI OF THE LIVER

Technical perspectives

Both 1.5T and 3T MRI devices have been used in liver DTI. Usually, a preliminary T2-weighted single-shot turbo spin echo sequence was required for anatomical localization. The coronal DTI was then acquired using the in-built single-shot echo planar imaging (EPI) sequence. Fat-saturation with the spectral adiabatic inversion recovery approach can be employed to avoid chemical-shift artefacts. Li *et al*[10] reported that good image quality, acceptable scan time and reasonable FA/ADC values were acquired using diffusion-encoding directions of 9 with *b*-value of 0.300 s/mm^2. The effect of respiratory and cardiac motion in liver DTI was assessed[11]. Although some study reported that respiratory motion tended to increase DTI metrics (mainly mean diffusivity), some researchers also suggest to acquire DTI during free breathing and to adjust respiratory mismatch by post-processing[12,13]. The left lobe appeared to present increased FA and mean diffusivity during systole, but the right lobe was less affected by cardiac motion[12]. Regarding the repeatability of diffusion-related parameters, both apparent diffusion coefficient (ADC, measured in DWI) and FA had relatively low degrees of variation on both intra-session and inter-session basis in general, but the right lobe values were considered more reliable than left lobes[11]. The normal images of hepatic DTI are presented in Figure 1.

DTI findings in livers with various pathologies

Diffusion studies in liver have been advocated as a tool to stage liver fibrosis, based on the assumption that fibrosis can be reflected by changes of diffusion properties. Whereas DWI is commonly used for such purposes, few studies reported DTI results. Two studies performed liver DTI on a 1.5T and a 3T scanner respectively, and both reported that conventional DWI performed better than DTI for the diagnosis of fibrosis and inflammation, and concluded that ADC values measured on DWI had the potential for fibrotic and inflammatory grading. The FA showed a trend toward higher levels with increasing inflammatory grade and fibrotic stage, but was of less diagnostic value. It was explained that many other non-specific pathologic processes could lead to FA elevation as well[14,15].

For focal mass-like lesions assessment, the literature is sparse. Erturk *et al*[16] reported that metastases tended to have low ADCs and high FA values, cysts had high
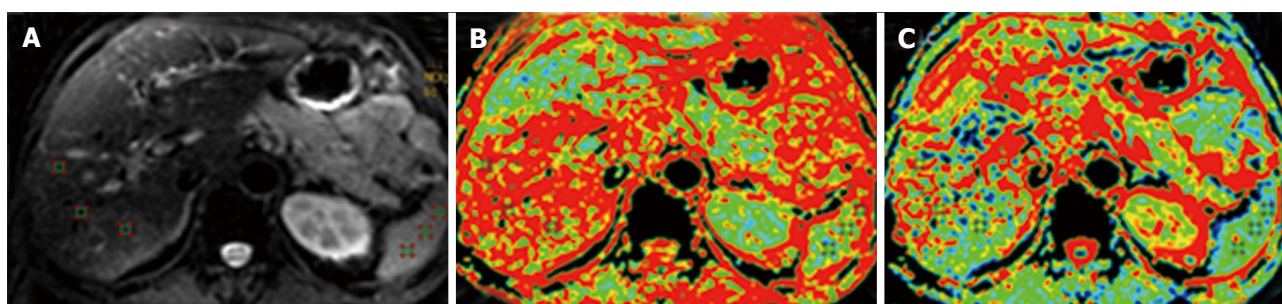
Figure 1 Normal images of hepatic diffusion tensor imaging. A: Diffusion image (*b* value of 0), mainly presenting the anatomic profiles; B: Fractional anisotropy map of the liver, presenting as the pseudo-colored image; C: Apparent diffusion coefficient map of the liver, presenting as the pseudo-colored image as well (Li *et al*[10], 2015; open access from *PlosOne*, permission confirmed).

ADCs and low FA values, and hemangiomas had high ADCs and high FA values. ADC had a better diagnostic performance for discriminating metastases from benign hepatic lesions than FA values (areas under the curve (Az values): 0.88 for ADC and 0.73 for FA), but FA had excellent ability to discriminate cysts from hemangiomas (Az value: 0.96)[16]. Another study revealed that hepatocellular carcinomas presented significantly lower ADC and higher mean FA value than normal liver regions, but diagnostic cutoff values, diagnostic accuracy and the comparison between ADC and FA were not given[10]. In general, DTI can play a supportive role in definition of focal liver lesion pathology.

DTI OF THE PANCREAS

The pancreas is a glandular organ with complex exocrine microstructure and endocrine microvascular physiology, and very few studies reported pancreatic DTI results. The normal images of pancreatic DTI are presented in Figure 2. A small sampled trial by Nissan *et al*[17] compared pancreatic DTI scans between healthy volunteers and patients with pancreatic-ductal-adenocacinoma. Fat-suppressed, respiratory triggered twice refocused spin-echo sequence, and *b*-values of 0, 100 and 500 s/mm^2 were used. They found a significant reduction in the directional diffusion coefficients and a lower contribution of fast intra-voxel-incoherent-motion (IVIM) component at $b \leqslant 100$ s/mm^2 in the malignant lesion[17].

Another larger sampled study focused on patients with acute pancreatitis (AP). It reported that both FA and ADC value from DTI could be employed to differentiate AP from normal pancreas, and also differentiate edema AP from necrosis AP. Furthermore, both ADC and FA value of pancreas had a negative correlation with the severity of AP (measured by MRI severity index). The authors discussed that the aggravation of pancreatic microcirculation ischemia, which played a key role in the transition from pancreatic edema to necrosis, could be detected by ADC and FA decreases[18]. DTI may spare the patients from radiation exposure of commonly used CT, and showed the potential to offer additional pathologic information to conventional MRI.

DTI OF THE KIDNEYS

Technical perspectives

Usually, a rapid T2-weighted sequence axial and coronal to the body axis were obtained for morphological evaluation. Then, coronal DTI were obtained with EPI. Several studies explored the optimal imaging parameters for anisotropy measurement. In the study of Kataoka *et al*[19], five different sequences with different parameters including respiration-triggered acquisition or multiple breath-holding, different slice thicknesses and different numbers of signal averaging and *b*-values were compared. It determined that the optimal sequence used respiratory triggering including a 3-mm slice thickness, three signal averages, and *b*-values of 0, 200 or 400 s/mm^2, which allowed the largest cortex–medulla difference of FA. Another study reported to have achieved high-resolution scans by free-breathing approaches, using a navigator-triggered sequence[20]. A later study registered DTI images of native and transplanted kidneys, using a multimodal nonrigid registration algorithm, and revealed that respiratory triggering was not necessary to measure diffusion parameters in transplanted kidneys, but still appeared advantageous in native kidneys[21]. However, these studies were small sampled, and based on the strategy to increase acquisition time, which lasted for 6 to 8 min and therefore the effect of respiratory motion needed to be properly handled. But some trials adopting shorter acquisition time appears reasonable to use breath-held, or even free-breathing approaches as well[22-24]. The influence of the number of encoding directions on image quality was explored; a preliminary study reported that the best image quality was visually assessed for images acquired with 15 and 32 encoding directions[25]. DTI at 1.5T and 3T were compared, researchers showed renal DTI with a 3T scanner had significant better signal to noise ratio (SNR) than that with a 1.5T scanner, although FA and ADCs at 3T did not significantly differ from that at 1.5T[26,27]. Indeed, increasing studies are using 3T systems to perform renal DTI.

Normal values and repeatability of renal DTI

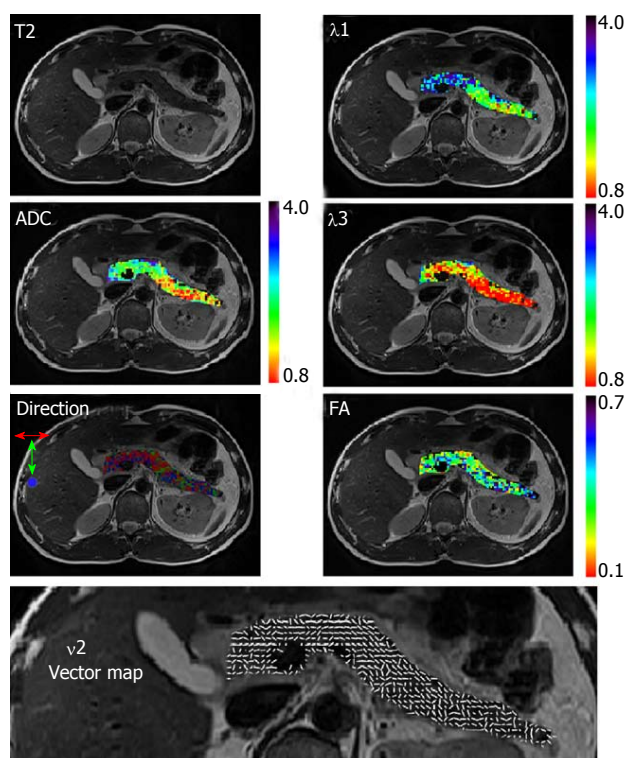In the renal structures, especially in the renal medulla,

Figure 2 Normal images of pancreatic diffusion tensor imaging. Maps were overlaid on the corresponding T2 weighted image. The direction map presents in three colors the direction of the 1st principal eigenvector; red: Left to right direction; green: Head to feet direction; and blue: Anterior to posterior direction. Vector map presents in white sticks the direction of the 1st principal eigenvector (Nissan *et al*[17], 2014; open access from *PlosOne*, permission confirmed). FA: Fractional anisotropy; ADC: Apparent diffusion coefficient.

diffusion properties are expected to be anisotropic as a consequence of the radial orientation of tubules, collecting ducts, and blood vessels, which are the basis for the application of DTI[28]. Indeed, kidney becomes the most explored organ to perform DTI among abdominal and pelvic structures up to date. The normal images of renal DTI are presented in Figure 3.

The medullary FA value (ranged from 0.32 to 0.45) was reported to be higher than the cortical FA value (ranged from 0.24 to 0.28), whereas the cortical ADC (ranged from 2.21 to 2.39 $\times$ 10^{-3} mm^2/s) was higher than the medullary ADC (ranged from 1.87 to 1.99 $\times$ 10^{-3} mm^2/s)[24,29,30]. This can be attributed to a more orientated architecture of the renal medulla than the cortex. One study reported that medullary FA values in women were lower than those in men, and medullary FA positively correlated with estimated glomerular filtration rate (eGFR)[29].

Repeatability is another issue concerned in clinical practice. Studies exhibited that the intra- and inter-observer measurements correlated well: No significant difference was noted between different observers, and the within-subject coefficient of variation obtained for both the ADC and FA values were less than 10% in the analyses[9,20,24]. Factors that may potentially influence the diffusion parameters include hydration status and

renal blood flow, *etc.* The study by Müller *et al*[31] showed significantly decreased ADC values in the kidneys of dehydrated healthy volunteers that increased upon rehydration, which could be attributed to the increase in GFR and osmotically driven water motion in the kidney. To reduce the inter-individual variation, fluid intake was suggested to be restricted prior to the scans. It has also been reported that ADC of the renal cortex and FA values of the renal medulla tended to elevate as the blood flow increased, which should be considered when interpreting DTI data[9].

DTI findings in kidneys with various pathologies
Diffused renal diseases such as chronic kidney disease usually lead to renal function impairment. Studies showed the feasibility of DTI to assess such conditions, inferring that the reduction of diffusion parameters was possibly caused by tubular atrophy, interstitial fibrosis, cellular infiltration, and the scarring of glomeruli. The parenchymal ADC and FA of kidneys was showed significantly lower in patients than healthy controls, regardless of whether eGFR was reduced. Both the renal ADC and FA values (both cortical and medullary) correlated with eGFR, and inversely correlated with serum creatinine and blood urea nitrogen[22,32]. Another article proposed the medullary FA value to be the main parameter for assessing renal function damage[33]. Relations between diffusion property changes and specific pathologic processes were investigated. The study of Liu *et al*[32] found that renal FA values (both cortical and medullary) negatively correlated with glomerular lesion and tubulointerstitial injury. Whereas another study investigating chronic glomerulonephritis concluded that cortical FA negatively correlated with the percentage of glomerulosclerosis, and medullary FA negatively correlated with tubulointerstitial fibrosis[34]. Some studies employed DTI to assess diabetic nephropathy (DN), reporting that both mean medullary FA and ADC were significantly lower in diabetics (even with eGFR > 60 mL/min per 1.73 m^2) than in controls, indicating the possibility of early identification of diabetics at risk of DN progression by DTI[35]. More recently, DTI was used to evaluate renal function in the follow-up of patients with autosomal dominant polycystic kidney disease[36].

For focal lesions in kidneys, the literature is sparse. A recent study used DTI to differentiate clear-cell renal cell carcinoma from low-fat renal angiomyolipomas (RAML). With the *b*-value of 0, 800 s/mm^2 and the cutoff FA value of 0.254, DTI reached a sensitivity of 100%, and a specificity of 73.3% for the differentiation[37]. However, other tumors were poorly reported so far.

DTI for the evaluation of transplanted kidneys
Renal transplantation has been established as the widely-accepted treatment for patients with end-stage renal diseases. Given the shortage of clinically available donor kidneys and the significant incidence of allograft dysfunction, noninvasive and accurate assessment of
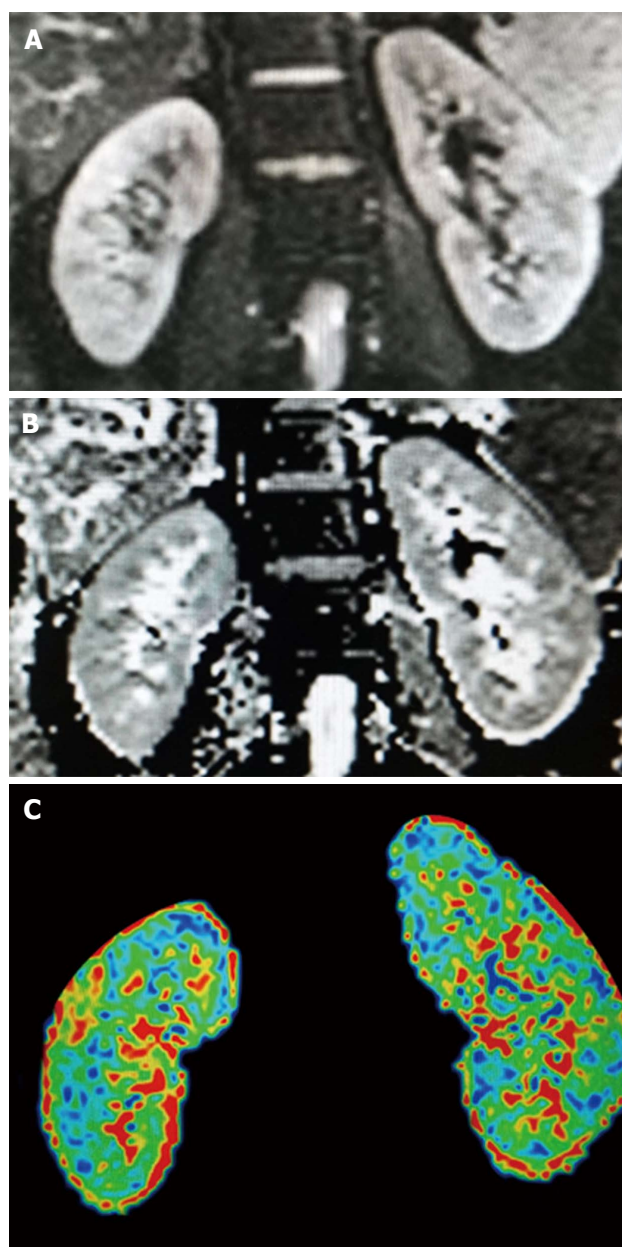
Figure 3 Normal images of renal diffusion tensor imaging. A: Diffusion image (*b*-value of 0), mainly presenting the anatomic profiles; B: Apparent diffusion coefficient map of the kidneys; C: Fractional anisotropy map of the kidneys, presenting as the pseudo-colored image.

the allograft renal function becomes critical to ensure the success of transplantation. Several studies explored the utility of DTI for the functional assessment. The medullary FA exhibited a high correlation with eGFR, and was proposed as a valuable indicator of allograft function[38,39]. Lanzman *et al*[38] also found that the corticomedullary difference in FA values was lower in functionally impaired renal allografts. Hueper *et al*[40] compared the DTI parameters between allografts with initial graft function and delayed graft function, and both FA and ADC exhibited an inverse correlation with the amount of renal fibrosis. These results indicated that DTI might become a sensitive biomarker of allograft function with the information of anisotropy.

DTI OF THE PROSTATE

Technical perspectives

The introduction of ultra-fast EPI sequences and parallel imaging techniques enabled the application of DTI to the prostate[41]. Both 1.5T and 3T scanners were used to perform prostatic DTI, but it is commonly accepted that 3T or even higher magnetic field systems can lead to higher SNR, improved spatial and temporal resolution[42]. Several different numbers of diffusion-encoding directions were tested, and all resulted satisfactory imaging quality in the study by Kim *et al*[43]. Reduced field-of-view acquisition was attempted in another study, generating high-resolution DTI of the prostate, which could potentially enable a more accurate detection of focal tumors[44].

Normal values of prostatic DTI

Prostate gland consists of various vascular, neural, and other anisotropic water paths, and there are distinct structural arrangements among central gland (CG), peripheral zone (PZ) and periprostatic neurovascular tracts, which make the DTI potentially applicable. Besides, the prostate is also an organ under the effect of the hormones and has dynamic changes as the age grows. In 2004, *in vivo* prostatic DTI were performed on six subjects, reporting a relatively high FA value of the PZ and CG of around 0.4. Later studies recorded lower FA values, and observed significant differences in the FA value between PZ (ranged from 0.16 to 0.21) and CZ (ranged from 0.26 to 0.37)[44,45]. Age-related changes of normal prostate were also assessed. The FA and ADC values in the normal prostatic PZ showed an age-dependent pattern, as FA decreases and ADC increases with age. Whereas the FA and ADC in CZ did not appear to be significantly age-related[46].

DTI for the diagnosis of prostate cancer and evaluation of periprostatic neurovascular bundles

Despite recent advances in MRI, the extent and aggressiveness of prostate cancer remain diagnostic challenges for radiologists. As the reliance on DWI increases in the clinical practice, DTI with additional anisotropic information was explored. An earlier study observed decreased FA values in the peripheral cancerous tissues compared with the normal peripheral portion[47]. Whereas no significant differences between the FA values for cancerous and normal PZ tissues in the study by Xu *et al*[48]. By contrast, later studies mostly reported increased FA values in cancerous tissues (ranged from 0.29 to 0.38) compared with non-cancerous tissues (ranged from 0.15 to 0.31), regardless of the location of the neoplastic tissue (either in PZ or CZ)[41,49,50]. Another study investigated the relation between gleason scores (GS) and DTI parameters in prostate cancer in PZ, revealing that FA values in the cancerous tissues were positively correlated with the GS (r = 0.48; P < 0.001), while the ADC values were negatively correlated with the GS (r = -0.54; P < 0.001)[51]. The authors claimed that increased FA were compatible with the hypercellular nature of prostate

tumors[52]. The variation in the FA values reported by the above-mentioned studies may be related to the different grades of malignant changes, as each study included relatively small sample with various cancer grades. In addition, Xu *et al*[48] discussed that the measured anisotropy could be biased with the increased image noise in the cancerous region where shorter T2 led to more significantly lowered SNR than in the normal regions. In general, the reliability of FA measurement still need to be improved, and DTI needs to be better integrated to multi-modality assessment of prostatic lesions.

Several studies investigated the evaluation of peri-prostatic neurovascular bundles by DTI, but the results varied. Some studies optimistically showed that 3D-DTI allowed effective description of the entire plexus of the periprostatic fibers in all directions[53,54]. But 3 of 8 subjects had no tracts detected with conventional DTI acquisition in another small-sampled study, in which zoomed DTI improved the detection rate[55]. A recent study even doubted whether the visualized DTI tracts really represent nerve tracts or neurovascular bundles, because DTI tract profiles were significantly dependent on FA thresholds and tended to present non-specificity[56]. Therefore, the utility of DTI for this indication remains controversial.

DTI OF THE UTERUS

The uterus is a fibromuscular organ with layered structures. The overall arrangement of muscle fibers is highly directional, which is the basis of DTI application. Specially, this organ is under the effect of hormones and has physiological (menstrual cycle, menopausal period) fluctuations, which may influence the diffusion properties. In 2006, three-dimensional fiber architecture of the normal human uterus based on DTI was evaluated in five samples *ex vivo*, revealing two basic fiber directions: Circular and longitudinal oriented[57]. The study by Fiocchi *et al*[58] confirmed such results *in vivo*, and showed that two third of the Caesarean-scarred uteri had altered fiber structure (lower fiber number and density) in the scarred anterior isthmus. They inferred that DTI may detect significant caesarean scars which may lead to subsequent placental complications. Diffusion of different layers were measured in the study by Fujimoto *et al*[59], showing that FA was the highest for junctional zone (0.297), followed by outer myometrium (0.257) and endometrium (0.186); fibers were the longest in outer myometrium (42.0 mm), followed by junctional zone (34.2 mm) and endometrium (20.0 mm). This presented detailed and quantified data for the understanding of the layered structure of uterus. The study by He *et al*[60] revealed that uterine FA and ADC values had dynamic changes during menstrual cycle, which includes several different phases: Menstrual phase (MP), follicular phase (FP), ovulatory phase (OP) and luteal phase (LP). Specifically, endometrial FA values significantly declined, whereas ADC values increased

during MP, and ADC values of myometrium significantly increased from MP to LP. Variation of FA values between MP-FP, MP-OP was found correlated moderately with serum oestradiol levels, and the authors inferred that higher serum oestradiol levels were accompanied by larger increase of the endometrium with higher isotropy of water diffusion directionality[60].

The DTI data of diseased uterus is quite scarce. Toba *et al*[61] investigated the feasibility of DTI for evaluating the myometrial invasion of endometrial cancer *ex vivo*. Myometrial infiltration of endometrial tumor may be detected with the disruption of the anisotropic layer, as the FA values of the tumors (0.21 ± 0.05) were significantly lower than the inner layer of the myometrial zone (0.44 ± 0.01) and exterior myometrium (0.32 ± 0.08)[61]. More pathologies need to be included to expand the understanding of DTI in uterus with abnormality.

DTI OF OTHER PELVIC STRUCTURES

DTI, especially with tractography, has been used to depict the fiber orientation of skeletal muscles to some extent. The female pelvic floor, which has a multilayered complex anatomy and includes several closely aligned muscles, were investigated by Zijta *et al*[62,63] with small samples. The assumption was to use DTI with fiber tractography to depict normal pelvic floor anatomy, and to further evaluate pelvic organ prolapse. Several clinically relevant pelvic structures (including the perineal body, anal sphincter complex, internal obturator muscle and the puboperineal muscle) were satisfactorily and reliably identified, but no significant differences in DTI parameters were found between the prolapse group and the asymptomatic group overall[62,63].

One study has investigated the anal canal structures by DTI so far. FA values of various layers of normal anal canal were measured, and good inter-rater agreement and test reproducibility were achieved[64]. However, further data remains lacked.

FUTURE DIRECTIONS OF RESEARCH

DTI scans of abdominal and pelvic organs still confront with technical limitations: Not only common issues related to abdominal and pelvic MRI such as motional artifacts due to breathing and peristalsis, but also additional problems related to DTI such as the low SNR of EPI sequence due to gradient eddy currents, B0 field inhomogeneity and susceptibility difference[17]. It seems state of art to balance the longer acquisition time and less motional artifacts by either improved sequence or motional triggering protocols. Further studies can explore better techniques to increase SNR, reduce geometrical distortions and assess the contribution of IVIM.

Another issue is the methodology of post-processing and parameter measurements, which would influence the reliability and repeatability of scan results. Factors influencing the DTI parameter measurements, such as

hydration state and blood flow of targeted organs, should be further understood in order to standardize patient conditions[24,65]. Besides, consensus is needed on the placement of regions of interest (ROIs), where mean FA was calculated, since ROIs were manually delineated along the outlines of the targeted organs in some studies, but were placed in representative regions of the organ or tissue in other studies[17,22].

In general, DTI is more applied in diffused diseases of solid organs than in focal lesions. Organs with more directionally arranged structures have been explored to a greater extent, such as the kidney. In the circumstances that DTI parameters such as FA was reported of less diagnostic value, it should be noted that the underlying pathologic conditions that led to a final presentation of disease (such as renal function impairment or liver fibrosis) can be heterogeneous[14,38]. Future studies can explore the potential of DTI to differentiate between these pathologic conditions.

In focal lesion assessment, it is suggested that FA might reflect the histology of tumors, in particular of tumor cell density, and it is expected that locations with higher FA would have higher tumor cellularity, as well as a relatively higher Ki-67 labeling index, and therefore a higher malignant potential[16,52,66]. Future studies could apply DTI in lesions with prominent cellularity changes. For example, it is known that the density of gastrointestinal stromal tumor metastases decrease after cytostatic chemotherapy, and FA might be shown of value in these group of patients[67].

The last but not the least, DTI scan should be further integrated into the current multi-modality evaluation in clinical practice. For instance, it is mentioned that the differentiation of hepatic masses such as cysts, hemangiomas, and metastases can be performed easily by well-established imaging criteria. In this regard, performing DTI might seem unnecessary[16]. Another example is the diagnosis of prostate cancer, where multi-modality functional imaging has been researched extensively. Combined algorithm can be designed in future studies with the purpose of a more precise and full-scaled assessment.

CONCLUSION

In conclusion, DTI has been explored and applied in abdominal and pelvic organs such as liver, pancreas, kidneys, prostate, uterus, *etc*. Technical advances enabled generally satisfactory image quality and measurement repeatability. DTI appears to be more valuable in the evaluation of diffused diseases of organs with highly directionally arranged structures, such as the assessment of function impairment of native and transplanted kidneys. However, the utility of DTI to diagnose focal lesions remains limited. It is suggested that DTI parameters might potentially depict certain pathologic characterization such as cell density. Furthermore, DTI should be better integrated into the current multi-modality evaluation in clinical practice.

REFERENCES

1   **Roditi G**, Maki JH, Oliveira G, Michaely HJ. Renovascular imaging in the NSF Era. *J Magn Reson Imaging* 2009; **30**: 1323-1334 [PMID: 19937926 DOI: 10.1002/jmri.21977]

2   **Notohamiprodjo M**, Reiser MF, Sourbron SP. Diffusion and perfusion of the kidney. *Eur J Radiol* 2010; **76**: 337-347 [PMID: 20580179 DOI: 10.1016/j.ejrad.2010.05.033]

3   **Pierpaoli C**, Basser PJ. Toward a quantitative assessment of diffusion anisotropy. *Magn Reson Med* 1996; **36**: 893-906 [PMID: 8946355 DOI: 10.1002/mrm.1910360612]

4   **Mori S**, van Zijl PC. Fiber tracking: principles and strategies - a technical review. *NMR Biomed* 2002; **15**: 468-480 [PMID: 12489096 DOI: 10.1002/nbm.781]

5   **Shenton ME**, Hamoda HM, Schneiderman JS, Bouix S, Pasternak O, Rathi Y, Vu MA, Purohit MP, Helmer K, Koerte I, Lin AP, Westin CF, Kikinis R, Kubicki M, Stern RA, Zafonte R. A review of magnetic resonance imaging and diffusion tensor imaging findings in mild traumatic brain injury. *Brain Imaging Behav* 2012; **6**: 137-192 [PMID: 22438191 DOI: 10.1007/s11682-012-9156-5]

6   **Sternberg EJ**, Lipton ML, Burns J. Utility of diffusion tensor imaging in evaluation of the peritumoral region in patients with primary and metastatic brain tumors. *AJNR Am J Neuroradiol* 2014; **35**: 439-444 [PMID: 24052506 DOI: 10.3174/ajnr.A3702]

7   **Hubbard EA**, Wetter NC, Sutton BP, Pilutti LA, Motl RW. Diffusion tensor imaging of the corticospinal tract and walking performance in multiple sclerosis. *J Neurol Sci* 2016; **363**: 225-231 [PMID: 27000254 DOI: 10.1016/j.jns.2016.02.044]

8   **Mürtz P**, Flacke S, Träber F, van den Brink JS, Gieseke J, Schild HH. Abdomen: diffusion-weighted MR imaging with pulse-triggered single-shot sequences. *Radiology* 2002; **224**: 258-264 [PMID: 12091693 DOI: 10.1148/radiol.2241011117]

9   **Cutajar M**, Clayden JD, Clark CA, Gordon I. Test-retest reliability and repeatability of renal diffusion tensor MRI in healthy subjects. *Eur J Radiol* 2011; **80**: e263-e268 [PMID: 21227619 DOI: 10.1016/j.ejrad.2010.12.018]

10   **Li X**, Liang Q, Zhuang L, Zhang X, Chen T, Li L, Liu J, Calimente H, Wei Y, Hu J. Preliminary Study of MR Diffusion Tensor Imaging of the Liver for the Diagnosis of Hepatocellular Carcinoma. *PLoS One* 2015; **10**: e0135568 [PMID: 26317346 DOI: 10.1371/journal.pone.0135568]

11   **Girometti R**, Maieron M, Lissandrello G, Bazzocchi M, Zuiani C. Test-retest reliability of diffusion tensor imaging of the liver at 3.0 T. *Radiol Med* 2015; **120**: 489-497 [PMID: 25421264 DOI: 10.1007/s11547-014-0479-8]

12   **Wong OL**, Gloh Lo G, Lee R, Wa Li W, Lung Chan P, Ki Yu S, Noseworthy MD. The effect of respiratory and cardiac motion in liver diffusion tensor imaging (DTI). *J Comput Assist Tomogr* 2014; **38**: 352-359 [PMID: 24681854 DOI: 10.1097/RCT.0000000000000064]

13   **Chen X**, Qin L, Pan D, Huang Y, Yan L, Wang G, Liu Y, Liang C, Liu Z. Liver diffusion-weighted MR imaging: reproducibility comparison of ADC measurements obtained with multiple breath-hold, free-breathing, respiratory-triggered, and navigator-triggered techniques. *Radiology* 2014; **271**: 113-125 [PMID: 24475860 DOI: 10.1148/radiol.13131572]

14   **Taouli B**, Chouli M, Martin AJ, Qayyum A, Coakley FV, Vilgrain V. Chronic hepatitis: role of diffusion-weighted imaging and diffusion tensor imaging for the diagnosis of liver fibrosis and inflammation. *J Magn Reson Imaging* 2008; **28**: 89-95 [PMID: 18581382 DOI: 10.1002/jmri.21227]

15   **Tosun M**, Inan N, Sarisoy HT, Akansel G, Gumustas S, Gürbüz Y, Demirci A. Diagnostic performance of conventional diffusion weighted imaging and diffusion tensor imaging for the liver fibrosis and inflammation. *Eur J Radiol* 2013; **82**: 203-207 [PMID: 23122674 DOI: 10.1016/j.ejrad.2012.09.009]

16   **Erturk SM**, Ichikawa T, Kaya E, Yapici O, Ozel A, Mahmutoglu AS, Basak M. Diffusion tensor imaging of cysts, hemangiomas, and metastases of the liver. *Acta Radiol* 2014; **55**: 654-660 [PMID: 24043882 DOI: 10.1177/0284185113504916]

17 **Nissan N**, Golan T, Furman-Haran E, Apter S, Inbar Y, Ariche A, Bar-Zakay B, Goldes Y, Schvimer M, Grobgeld D, Degani H. Diffusion tensor magnetic resonance imaging of the pancreas. *PLoS One* 2014; **9**: e115783 [PMID: 25549366 DOI: 10.1371/journal.pone.0115783]

18 **Li X**, Zhuang L, Zhang X, Wang J, Chen T, Li L, Aduah EA, Hu J. Preliminary Study of MR Diffusion Tensor Imaging of Pancreas for the Diagnosis of Acute Pancreatitis. *PLoS One* 2016; **11**: e0160115 [PMID: 27584016 DOI: 10.1371/journal.pone.0160115]

19 **Kataoka M**, Kido A, Yamamoto A, Nakamoto Y, Koyama T, Isoda H, Maetani Y, Umeoka S, Tamai K, Saga T, Morisawa N, Mori S, Togashi K. Diffusion tensor imaging of kidneys with respiratory triggering: optimization of parameters to demonstrate anisotropic structures on fraction anisotropy maps. *J Magn Reson Imaging* 2009; **29**: 736-744 [PMID: 19243070 DOI: 10.1002/jmri.21669]

20 **Chan RW**, Von Deuster C, Stoeck CT, Harmer J, Punwani S, Ramachandran N, Kozerke S, Atkinson D. High-resolution diffusion tensor imaging of the human kidneys using a free-breathing, multi-slice, targeted field of view approach. *NMR Biomed* 2014; **27**: 1300-1312 [PMID: 25219683 DOI: 10.1002/nbm.3190]

21 **Seif M**, Mani LY, Lu H, Boesch C, Reyes M, Vogt B, Vermathen P. Diffusion tensor imaging of the human kidney: Does image registration permit scanning without respiratory triggering? *J Magn Reson Imaging* 2016; **44**: 327-334 [PMID: 26871263 DOI: 10.1002/jmri.25176]

22 **Wang WJ**, Pui MH, Guo Y, Wang LQ, Wang HJ, Liu M. 3T magnetic resonance diffusion tensor imaging in chronic kidney disease. *Abdom Imaging* 2014; **39**: 770-775 [PMID: 24623033 DOI: 10.1007/s00261-014-0116-y]

23 **Thoeny HC**, De Keyzer F, Oyen RH, Peeters RR. Diffusion-weighted MR imaging of kidneys in healthy volunteers and patients with parenchymal diseases: initial experience. *Radiology* 2005; **235**: 911-917 [PMID: 15845792 DOI: 10.1148/radiol.2353040554]

24 **Gürses B**, Kiliçkesmez O, Taşdelen N, Firat Z, Gürmen N. Diffusion tensor imaging of the kidney at 3 Tesla MRI: normative values and repeatability of measurements in healthy volunteers. *Diagn Interv Radiol* 2011; **17**: 317-322 [PMID: 21108183]

25 **Chuck NC**, Steidle G, Blume I, Fischer MA, Nanz D, Boss A. Diffusion Tensor Imaging of the Kidneys: Influence of b-Value and Number of Encoding Directions on Image Quality and Diffusion Tensor Parameters. *J Clin Imaging Sci* 2013; **3**: 53 [PMID: 24404412 DOI: 10.4103/2156-7514.122323]

26 **Kido A**, Kataoka M, Yamamoto A, Nakamoto Y, Umeoka S, Koyama T, Maetani Y, Isoda H, Tamai K, Morisawa N, Saga T, Mori S, Togashi K. Diffusion tensor MRI of the kidney at 3.0 and 1.5 Tesla. *Acta Radiol* 2010; **51**: 1059-1063 [PMID: 20735277 DOI: 10.3109/02841851.2010.504741]

27 **Notohamiprodjo M**, Dietrich O, Horger W, Horng A, Helck AD, Herrmann KA, Reiser MF, Glaser C. Diffusion tensor imaging (DTI) of the kidney at 3 tesla-feasibility, protocol evaluation and comparison to 1.5 Tesla. *Invest Radiol* 2010; **45**: 245-254 [PMID: 20375845 DOI: 10.1097/RLI.0b013e3181d83abc]

28 **Ries M**, Jones RA, Basseau F, Moonen CT, Grenier N. Diffusion tensor MRI of the human kidney. *J Magn Reson Imaging* 2001; **14**: 42-49 [PMID: 11436213 DOI: 10.1002/jmri.1149]

29 **Zheng Z**, Shi H, Zhang J, Zhang Y. Renal water molecular diffusion characteristics in healthy native kidneys: assessment with diffusion tensor MR imaging. *PLoS One* 2014; **9**: e113469 [PMID: 25470776 DOI: 10.1371/journal.pone.0113469]

30 **Wang WJ**, Pui MH, Guo Y, Hu XS, Wang HJ, Yang D. MR diffusion tensor imaging of normal kidneys. *J Magn Reson Imaging* 2014; **40**: 1099-1102 [PMID: 24925441 DOI: 10.1002/jmri.24450]

31 **Müller MF**, Prasad PV, Bimmler D, Kaiser A, Edelman RR. Functional imaging of the kidney by means of measurement of the apparent diffusion coefficient. *Radiology* 1994; **193**: 711-715 [PMID: 7972811 DOI: 10.1148/radiology.193.3.7972811]

32 **Liu Z**, Xu Y, Zhang J, Zhen J, Wang R, Cai S, Yuan X, Liu Q. Chronic kidney disease: pathological and functional assessment with diffusion tensor imaging at 3T MR. *Eur Radiol* 2015; **25**: 652-660 [PMID: 25304821 DOI: 10.1007/s00330-014-3461-x]

33 **Gaudiano C**, Clementi V, Busato F, Corcioni B, Orrei MG, Ferramosca E, Fabbri E, Berardi P, Santoro A, Golfieri R. Diffusion tensor imaging and tractography of the kidneys: assessment of chronic parenchymal diseases. *Eur Radiol* 2013; **23**: 1678-1685 [PMID: 23300038 DOI: 10.1007/s00330-012-2749-y]

34 **Feng Q**, Ma Z, Wu J, Fang W. DTI for the assessment of disease stage in patients with glomerulonephritis--correlation with renal histology. *Eur Radiol* 2015; **25**: 92-98 [PMID: 25038861 DOI: 10.1007/s00330-014-3336-1]

35 **Lu L**, Sedor JR, Gulani V, Schelling JR, O'Brien A, Flask CA, MacRae Dell K. Use of diffusion tensor MRI to identify early changes in diabetic nephropathy. *Am J Nephrol* 2011; **34**: 476-482 [PMID: 22024476 DOI: 10.1159/000333044]

36 **Lupica R**, Mormina E, Lacquaniti A, Trimboli D, Bianchimano B, Marino S, Bramanti P, Longo M, Buemi M, Granata F. 3 Tesla-Diffusion Tensor Imaging in Autosomal Dominant Polycystic Kidney Disease: The Nephrologist's Point of View. *Nephron* 2016; **134**: 73-80 [PMID: 27504997 DOI: 10.1159/000442296]

37 **Feng Q**, Ma Z, Zhang S, Wu J. Usefulness of diffusion tensor imaging for the differentiation between low-fat angiomyolipoma and clear cell carcinoma of the kidney. *Springerplus* 2016; **5**: 12 [PMID: 26759751 DOI: 10.1186/s40064-015-1627-x]

38 **Lanzman RS**, Ljimani A, Pentang G, Zgoura P, Zenginli H, Kröpil P, Heusch P, Schek J, Miese FR, Blondin D, Antoch G, Wittsack HJ. Kidney transplant: functional assessment with diffusion-tensor MR imaging at 3T. *Radiology* 2013; **266**: 218-225 [PMID: 23169797 DOI: 10.1148/radiol.12112522]

39 **Fan WJ**, Ren T, Li Q, Zuo PL, Long MM, Mo CB, Chen LH, Huang LX, Shen W. Assessment of renal allograft function early after transplantation with isotropic resolution diffusion tensor imaging. *Eur Radiol* 2016; **26**: 567-575 [PMID: 26017738 DOI: 10.1007/s00330-015-3841-x]

40 **Hueper K**, Khalifa AA, Bräsen JH, Vo Chieu VD, Gutberlet M, Wintterle S, Lehner F, Richter N, Peperhove M, Tewes S, Weber K, Haller H, Wacker F, Gwinner W, Gueler F, Hartung D. Diffusion-Weighted imaging and diffusion tensor imaging detect delayed graft function and correlate with allograft fibrosis in patients early after kidney transplantation. *J Magn Reson Imaging* 2016; **44**: 112-121 [PMID: 26778459 DOI: 10.1002/jmri.25158]

41 **Gürses B**, Kabakci N, Kovanlikaya A, Firat Z, Bayram A, Uluğ AM, Kovanlikaya I. Diffusion tensor imaging of the normal prostate at 3 Tesla. *Eur Radiol* 2008; **18**: 716-721 [PMID: 17960389 DOI: 10.1007/s00330-007-0795-7]

42 **Kim CK**, Park BK. Update of prostate magnetic resonance imaging at 3 T. *J Comput Assist Tomogr* 2008; **32**: 163-172 [PMID: 18379296 DOI: 10.1097/RCT.0b013e3180683b99]

43 **Kim CK**, Jang SM, Park BK. Diffusion tensor imaging of normal prostate at 3 T: effect of number of diffusion-encoding directions on quantitation and image quality. *Br J Radiol* 2012; **85**: e279-e283 [PMID: 21896666 DOI: 10.1259/bjr/21316959]

44 **Reischauer C**, Wilm BJ, Froehlich JM, Gutzeit A, Prikler L, Gablinger R, Boesiger P, Wentz KU. High-resolution diffusion tensor imaging of prostate cancer using a reduced FOV technique. *Eur J Radiol* 2011; **80**: e34-e41 [PMID: 20638208 DOI: 10.1016/j.ejrad.2010.06.038]

45 **Li C**, Chen M, Li S, Zhao X, Zhang C, Liu M, Zhou C. Diffusion tensor imaging of prostate at 3.0 Tesla. *Acta Radiol* 2011; **52**: 813-817 [PMID: 21586608 DOI: 10.1258/ar.2011.100487]

46 **Zhang J**, Tian WZ, Hu CH, Niu TL, Wang XL, Chen XY. Age-related changes of normal prostate: evaluation by MR diffusion tensor imaging. *Int J Clin Exp Med* 2015; **8**: 11220-11224 [PMID: 26379927]

47 **Manenti G**, Carlani M, Mancino S, Colangelo V, Di Roma M, Squillaci E, Simonetti G. Diffusion tensor magnetic resonance imaging of prostate cancer. *Invest Radiol* 2007; **42**: 412-419 [PMID: 17507813 DOI: 10.1097/01.rli.0000264059.46444.bf]

48 **Xu J**, Humphrey PA, Kibel AS, Snyder AZ, Narra VR, Ackerman JJ, Song SK. Magnetic resonance diffusion characteristics of histologically defined prostate cancer in humans. *Magn Reson Med* 2009; **61**: 842-850 [PMID: 19215051 DOI: 10.1002/mrm.21896]

49 **Li C**, Chen M, Li S, Zhao X, Zhang C, Luo X, Zhou C. Detection of prostate cancer in peripheral zone: comparison of MR diffusion tensor imaging, quantitative dynamic contrast-enhanced MRI, and the two techniques combined at 3.0 T. *Acta Radiol* 2014; **55**: 239-247 [PMID: 23892233 DOI: 10.1177/0284185113494978]

50 **Park SY**, Kim CK, Park BK, Ha SY, Kwon GY, Kim B. Diffusion-tensor MRI at 3 T: differentiation of central gland prostate cancer from benign prostatic hyperplasia. *AJR Am J Roentgenol* 2014; **202**: W254-W262 [PMID: 24555622 DOI: 10.2214/AJR.13.11015]

51 **Li L**, Margolis DJ, Deng M, Cai J, Yuan L, Feng Z, Min X, Hu Z, Hu D, Liu J, Wang L. Correlation of gleason scores with magnetic resonance diffusion tensor imaging in peripheral zone prostate cancer. *J Magn Reson Imaging* 2015; **42**: 460-467 [PMID: 25469909 DOI: 10.1002/jmri.24813]

52 **Gürses B**, Tasdelen N, Yencilek F, Kılıckesmez NO, Alp T, Fırat Z, Albayrak MS, Uluğ AM, Gürmen AN. Diagnostic utility of DTI in prostate cancer. *Eur J Radiol* 2011; **79**: 172-176 [PMID: 20138721 DOI: 10.1016/j.ejrad.2010.01.009]

53 **Panebianco V**, Barchetti F, Sciarra A, Marcantonio A, Zini C, Salciccia S, Collettini F, Gentile V, Hamm B, Catalano C. In vivo 3D neuroanatomical evaluation of periprostatic nerve plexus with 3T-MR Diffusion Tensor Imaging. *Eur J Radiol* 2013; **82**: 1677-1682 [PMID: 23773553 DOI: 10.1016/j.ejrad.2013.05.013]

54 **Finley DS**, Ellingson BM, Natarajan S, Zaw TM, Raman SS, Schulam P, Reiter RE, Margolis D. Diffusion tensor magnetic resonance tractography of the prostate: feasibility for mapping periprostatic fibers. *Urology* 2012; **80**: 219-223 [PMID: 22748877 DOI: 10.1016/j.urology.2012.03.027]

55 **Ream JM**, Glielmi C, Lazar M, Campbell N, Pfeuffer J, Schneider R, Rosenkrantz AB. Zoomed echo-planar diffusion tensor imaging for MR tractography of the prostate gland neurovascular bundle without an endorectal coil: a feasibility study. *Abdom Radiol* (NY) 2016; **41**: 919-925 [PMID: 27193790 DOI: 10.1007/s00261-015-0587-5]

56 **Baur AD**, Daqqaq T, Collettini F, Denecke T, Hamm B, Durmus T, Scheel M. Influence of fractional anisotropy thresholds on diffusion tensor imaging tractography of the periprostatic neurovascular bundle and selected pelvic tissues: do visualized tracts really represent nerves? *Acta Radiol* 2017; **58**: 472-480 [PMID: 27235453]

57 **Weiss S**, Jaermann T, Schmid P, Staempfli P, Boesiger P, Niederer P, Caduff R, Bajka M. Three-dimensional fiber architecture of the nonpregnant human uterus determined ex vivo using magnetic resonance diffusion tensor imaging. *Anat Rec A Discov Mol Cell Evol Biol* 2006; **288**: 84-90 [PMID: 16345078 DOI: 10.1002/ar.a.20274]

58 **Fiocchi F**, Nocetti L, Siopis E, Currà S, Costi T, Ligabue G, Torricelli P. In vivo 3 T MR diffusion tensor imaging for detection of the fibre architecture of the human uterus: a feasibility and quantitative study. *Br J Radiol* 2012; **85**: e1009-e1017 [PMID: 22744322 DOI: 10.1259/bjr/76693739]

59 **Fujimoto K**, Kido A, Okada T, Uchikoshi M, Togashi K. Diffusion tensor imaging (DTI) of the normal human uterus in vivo at 3 tesla: comparison of DTI parameters in the different uterine layers. *J Magn Reson Imaging* 2013; **38**: 1494-1500 [PMID: 23576451 DOI: 10.1002/jmri.24114]

60 **He Y**, Ding N, Li Y, Li Z, Xiang Y, Jin Z, Xue H. 3-T diffusion tensor imaging (DTI) of normal uterus in young and middle-aged females during the menstrual cycle: evaluation of the cyclic changes of fractional anisotropy (FA) and apparent diffusion coefficient (ADC) values. *Br J Radiol* 2015; **88**: 20150043 [PMID: 25785919 DOI: 10.1259/bjr.20150043]

61 **Toba M**, Miyasaka N, Sakurai U, Yamada I, Eishi Y, Kubota T. Diagnostic possibility of diffusion tensor imaging for the evaluation of myometrial invasion in endometrial cancer: an ex vivo study. *J Magn Reson Imaging* 2011; **34**: 616-622 [PMID: 21751283 DOI: 10.1002/jmri.22693]

62 **Zijta FM**, Froeling M, van der Paardt MP, Lakeman MM, Bipat S, van Swijndregt AD, Strijkers GJ, Nederveen AJ, Stoker J. Feasibility of diffusion tensor imaging (DTI) with fibre tractography of the normal female pelvic floor. *Eur Radiol* 2011; **21**: 1243-1249 [PMID: 21197534 DOI: 10.1007/s00330-010-2044-8]

63 **Zijta FM**, Lakeman MM, Froeling M, van der Paardt MP, Borstlap CS, Bipat S, Montauban van Swijndregt AD, Strijkers GJ, Roovers JP, Nederveen AJ, Stoker J. Evaluation of the female pelvic floor in pelvic organ prolapse using 3.0-Tesla diffusion tensor imaging and fibre tractography. *Eur Radiol* 2012; **22**: 2806-2813 [PMID: 22797954 DOI: 10.1007/s00330-012-2548-5]

64 **Goh V**, Tam E, Taylor NJ, Stirling JJ, Simcock IC, Jones RG, Padhani AR. Diffusion tensor imaging of the anal canal at 3 tesla: feasibility and reproducibility of anisotropy measures. *J Magn Reson Imaging* 2012; **35**: 820-826 [PMID: 22127778 DOI: 10.1002/jmri.22873]

65 **Heusch P**, Wittsack HJ, Kröpil P, Blondin D, Quentin M, Klasen J, Pentang G, Antoch G, Lanzman RS. Impact of blood flow on diffusion coefficients of the human kidney: a time-resolved ECG-triggered diffusion-tensor imaging (DTI) study at 3T. *J Magn Reson Imaging* 2013; **37**: 233-236 [PMID: 22807237 DOI: 10.1002/jmri.23751]

66 **Kinoshita M**, Hashimoto N, Goto T, Kagawa N, Kishima H, Izumoto S, Tanaka H, Fujita N, Yoshimine T. Fractional anisotropy and tumor cell density of the tumor core show positive correlation in diffusion tensor magnetic resonance imaging of malignant brain tumors. *Neuroimage* 2008; **43**: 29-35 [PMID: 18672074 DOI: 10.1016/j.neuroimage.2008.06.041]

67 **Choi H**, Charnsangavej C, de Castro Faria S, Tamm EP, Benjamin RS, Johnson MM, Macapinlac HA, Podoloff DA. CT evaluation of the response of gastrointestinal stromal tumors after imatinib mesylate treatment: a quantitative analysis correlated with FDG PET findings. *AJR Am J Roentgenol* 2004; **183**: 1619-1628 [PMID: 15547201 DOI: 10.2214/ajr.183.6.01831619]